Evaluation of pressure and force after dam break using weakly compressible SPH

Petr Jančík*[1], Supervisors: Pavel Šafařík[1], Tomáš Hyhlík[1]

[1] *Department of Fluid Dynamics and Thermodynamics, Faculty of Mechanical Engineering, Czech Technical University in Prague, Technická 4, 166 07 Prague 6, Czech Republic*

Abstract

This paper presents a solution of a dam break flow over a dry horizontal bed in two dimensions using the weakly compressible smoothed particle hydrodynamics (SPH) method. This work focuses mainly on the evaluation of pressure and forces exerted on the downstream vertical wall. First, a pressure evaluation technique suitable for weakly compressible SPH is described. Validation of the technique using experimental data follows, and finally, the pressure distribution and the total force on the vertical wall is evaluated. Analysis of pressure distribution and total force as a function of time is carried out. All physical quantities are converted into non-dimensional variables for simple comparison with results in other works.

Key-words: dam collapse; pressure evaluation; free surface; SPH; CFD

1. Introduction

A column of liquid released from a tank by sudden removing of one of its walls offers a varied palette of phenomena to be studied, and it is quite impressive from the visual point of view. These might be the main reason why it has been investigated so many times in many different modifications and by many different approaches and methods.

The authors most often focus on the kinematics of the flow. The fundamental experimental work on this topic by Martin et al. was dealing with the surge front position and the height of the column as a function of time [1]. Experimental kinematic data were used for validation of numerical methods for free surface flow, e.g., the volume of fluid for finite volume method [2], smoothed particle hydrodynamics [3], or moving-particle semi-implicit [4].

Not only kinematic behaviour but also dynamic effects were taken into account recently. Pressure values on vertical downstream wall impacted by the surge were measured in different heights by Zhou et al. [5], Kleefsman et al. [6], or Wemmenhove et al. [7]. All these works have been used for verification of numerical methods for free surface flow. Lobovský et al. [8] located the pressure sensors so, that the positions matched with the set-ups from the previously mentioned works and compared the results. Pressure and forces were evaluated for validation of SPH models as well, e.g., Marrone et al. [9] and Adami et al. [10]. Data from [5] were used in both these cases.

In recent works by the author, kinematics of the solution obtained with the presented SPH method was proved to be in agreement with experimental data [11, 12]. Therefore, this paper focuses on the dynamics of the flow. The first goal of this work is to validate the proposed pressure evaluation technique for weakly compressible SPH using experimental data from [8]. The subsequent goal is to use this technique to evaluate pressure on the downstream vertical wall after the surge impact and total pressure load. The following analysis identifies interesting or important moments of the process and links them with flow kinematics.

*Corresponding author: Petr.Jancik@fs.cvut.cz

2. Method

2.1. Weakly compressible SPH

Smoothed particle hydrodynamics is a mesh-free particle method. Its Lagrangian nature makes it particularly suitable for transient multiphase problems. A very brief description of the method with emphasis on parts influencing pressure evaluation is given in the following paragraphs. For more detailed information see for example [13].

One of the key concepts of the SPH is so-called weight function. In this work, truncated Gaussian function is employed. It is usually written as

$$W(R,h) = \begin{cases} \pi^{-\frac{d}{2}} h^{-d} e^{-R^2} & \text{if } R < 3 \\ 0 & \text{if } R \geq 3 \end{cases} , \quad (1)$$

where h is so-called smoothing length, d is number of spatial dimensions, and $R = |\vec{x}_j - \vec{x}_i|/h$. Vector $\vec{x}$ is spatial coordinate and indices i and j denote interacting particles.

The governing equations of compressible and inviscid fluid motion in SPH discretized form are

$$\frac{\mathrm{D}\varrho_i}{\mathrm{D}t} = \varrho_i \sum_j \frac{m_j}{\varrho_j} (\vec{v}_i - \vec{v}_j) \cdot \nabla W_{ij} + D_i \, , \quad (2)$$

$$\frac{\mathrm{D}\vec{v}_i}{\mathrm{D}t} = -\sum_j m_j \Big(\frac{p_j}{\varrho_j^2} + \frac{p_i}{\varrho_i^2} + \Pi_{ij} \Big) \nabla W_{ij} + \vec{f}_i \, , \quad (3)$$

where ϱ, $\vec{v}$, p, m, and t denote density, velocity, pressure, mass, and time. Other symbols $\vec{f}$, Π, and D are the intensity of external body force, artificial viscosity term, and artificial mass diffusion term.

Since the fluid is modelled as compressible, an equation of state is needed to close the system of equations. A popular choice is equation in the form

$$p = \frac{c^2 \varrho_0}{\gamma} \left[\left(\frac{\rho}{\varrho_0} \right)^{\gamma} - 1 \right] , \quad (4)$$

where c is speed of sound, ϱ_0 is reference density, and γ is exponent of the equation. Exponent $\gamma = 7$ is usually chosen for liquids. The speed of sound could be set to its actual physical value, but this choice would demand very small time steps. Maximal time step for numerical stability of an explicit integration scheme is indirectly proportional to the speed of sound. Therefore, a good choice proved to be a value about ten times higher than the maximal velocity of the flow, which keeps the fluid almost incompressible while the integration is reasonably effective [3].

Artificial viscosity term is commonly used Monaghan artificial viscosity which ensures numerical stability [14]. Artificial mass diffusion smooths density field, which is naturally very noisy in weakly compressible SPH. It can be written as

$$D_i = 2\delta hc \sum_j (\varrho_j - \varrho_i) \frac{(\vec{x}_j - \vec{x}_i) \cdot \nabla W_{ij}}{(\vec{x}_i - \vec{x}_j) \cdot (\vec{x}_i - \vec{x}_j)} , \quad (5)$$

where δ is a coefficient of artificial diffusion [15].

The artificial diffusion would not smooth density field enough for correct pressure evaluation. An additional density field smoothing technique is therefore employed. It is density reinitialization and it is described by the formula

$$\varrho_i = \frac{\sum_j m_j W_{ij}}{\sum_j \frac{m_j}{\varrho_j} W_{ij}} . \quad (6)$$

It is performed every twenty time steps. Similar technique applied Colagrossi and Landrini [16].

Wall boundary condition is modelled as free-slip, and the same dummy particle method was used as in previous work [12]. This method preserves the pressure field near the walls sufficiently smooth. Free surface is formed naturally thanks to Lagrangian nature of the SPH method and appropriate choice of the equation of state.

2.2. Pressure and force evaluation

Each particle has its own pressure value, and it changes its position in time. However, we need to obtain pressure value at a certain point fixed in space. Pressure value at this point is obtained by interpolation from neighbouring fluid particles using formula

$$p_S = \frac{\sum_j p_j W_{Sj}}{\sum_j W_{Sj}} , \quad (7)$$

where index S denotes pressure sensor. Smoothing length is chosen the same as for the simulation itself. Too high value of the smoothing length would lead to too distant particles to be considered, and the result would be incorrect. The same applies for too low value because not enough particles would be taken into account.

Small groups of particles detach from the main fluid body. Pressure values of particles in these groups are erroneous. That is a particle count threshold is defined. Pressure reading is carried out only if the number of particles influencing the sensor is above this threshold. An appropriate value appears to be 50% of the maximal potential number of influencing particles.

The pressure signal from the sensor is still very noisy, and high frequencies have to be suppressed. As a low-pass filter is used weight function in the time domain where $d = 1$ and smoothing length h is replaced by smoothing time period τ. Choice of this period is problem dependent. It has to suppress numerical noise but should not smooth out physical phenomena. The time filtering can be written

$$p_{Sm} = \frac{\sum_n p_{Sn} W_{mn}}{\sum_n W_{mn}} , \quad (8)$$

where indices m and n denote time steps. Moreover, correct sampling has to be kept in mind because aliasing can occur. Reading the pressure value every fifth integration step, proved to be sufficient to capture the highest frequencies in the signal.

The total force acting on a wall is a sum of pressure values multiplied by the corresponding areas of the pressure sensors. In mathematical notation this is

$$\vec{F} = \sum_S p_S \vec{A}_S . \quad (9)$$

The area A_S is dependent on a distribution of the sensors. Distances between the sensors are chosen the same as the initial fluid particle spacing.

3. Results

3.1. Problem description

The solved problem corresponds to the experimental apparatus used in [8]. The numerical solution is performed in two dimensions and all important dimensions including the placement of pressure sensors P1-P4 displays Figure 1.

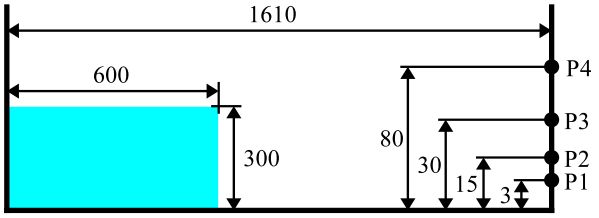

Fig. 1. *Scheme of the problem with positions of the pressure sensors. Dimensions in millimetres.*

The fluid domain is divided into 20 000 identical particles. A solution using a coarser resolution was computed as well. There was virtually no difference in the kinematics of the flow, but pressure values were slightly different because the size of the domain of influence of a pressure sensor is resolution dependent.

For the sake of easier comparison with other experimental or numerical results, non-dimensional variables are defined and used from now on. Non-dimensional time, vertical dimension, pressure, and force are defined as

$$T = t\sqrt{\frac{|\vec{g}|}{y_0}} , \quad (10)$$

$$Y = \frac{y}{y_0} , \quad (11)$$

$$P = \frac{p}{\varrho_0 |\vec{g}| y_0} , \quad (12)$$

$$\Phi = \frac{2|\vec{F}|}{\varrho_0 |\vec{g}| y_0^2 z_0} , \quad (13)$$

where $\vec{g}$ is the gravity acceleration vector, y_0 is the initial liquid column height, and z_0 is the width of the column, which is unity in a two-dimensional case. Definition of non-dimensional force gives unity value for a hydrostatic load on a rectangular vertical wall of height $y_0 = 300$ mm.

3.2. Validation of the pressure evaluation method

Four pressure sensors P1 - P4 are placed on the vertical wall at non-dimensional height 0.01, 0.05, 0.1, and 0.267 respectively. Pressure values as functions of time at these given points were evaluated and compared with the experimental results from [8]. Both experimental and numerical data are plotted in Figure 2.

In the experiment, the highest pressure value occurs at the lowest sensor P1 immediately after the surge impact, and the pressure value drops afterwards. Two higher sensors P2 and P3 give lower maximal pressure, and these peaks are not as sharp as the first one. Furthermore, they are slightly shifted towards later times. The fourth sensor shows a gradual pressure rise without a noticeable peak. The pressure at all four sensors rises again slightly at about $T = 5.8$. This rise is caused by the impact of the rolling wave, which emerges during the process.

Peak value at P1 is slightly overestimated, while maximal value at P3 is predicted lower than the experimental value. The pressure at P4 rises slower, but it reaches the experimental value at about $T = 4.5$. Increase in pressure caused by the rolling wave impact is noticeable as well. However, it occurs later than in the experiment.

The qualitative agreement of numerical and experimental data is very good overall; all the important phenomena are captured properly. From the quantitative point of view, the result is good. The difference between the simulation and the experiment does not exceed 15% for sensors P1 - P3. The worst level of agreement is for the highest sensor P4; the difference is up to 50%. Overall, pressure data obtained from the simulation can be used to predict pressure load, at least from a qualitative perspective.

3.3. Evaluation of pressure distribution and force

Total non-dimensional force on the downstream vertical wall as a function of non-dimensional time displays Figure 3. Pressure distribution as a function of time in non-dimensional variables shows Figure 4.

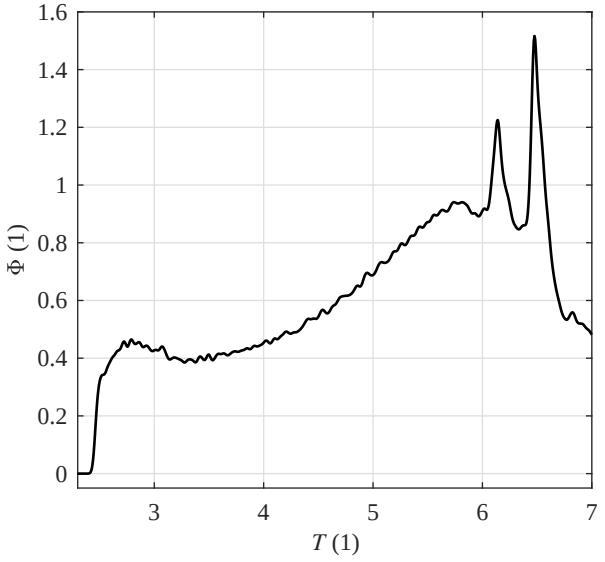

Fig. 3. *Non-dimensional force acting on the downstream vertical wall as a function of non-dimensional time.*

Maximal pressure value occurs immediately after the initial impact ($T = 2.48$), and it is limited to a very small area near the bottom of the wall (Figure 5). Its magnitude is almost four times bigger than hydrostatic pressure caused by a liquid column of the initial height. The total force is influenced by two major factors. The first one is the maximal pressure value in the corner of the tank, and the other is the overall area of the wall affected by the liquid. The pressure peak gradually vanishes while the overall area affected by the liquid increases as the thickness of the liquid layer impacting the wall grows and a jet is formed along the wall. As a result, a peak of

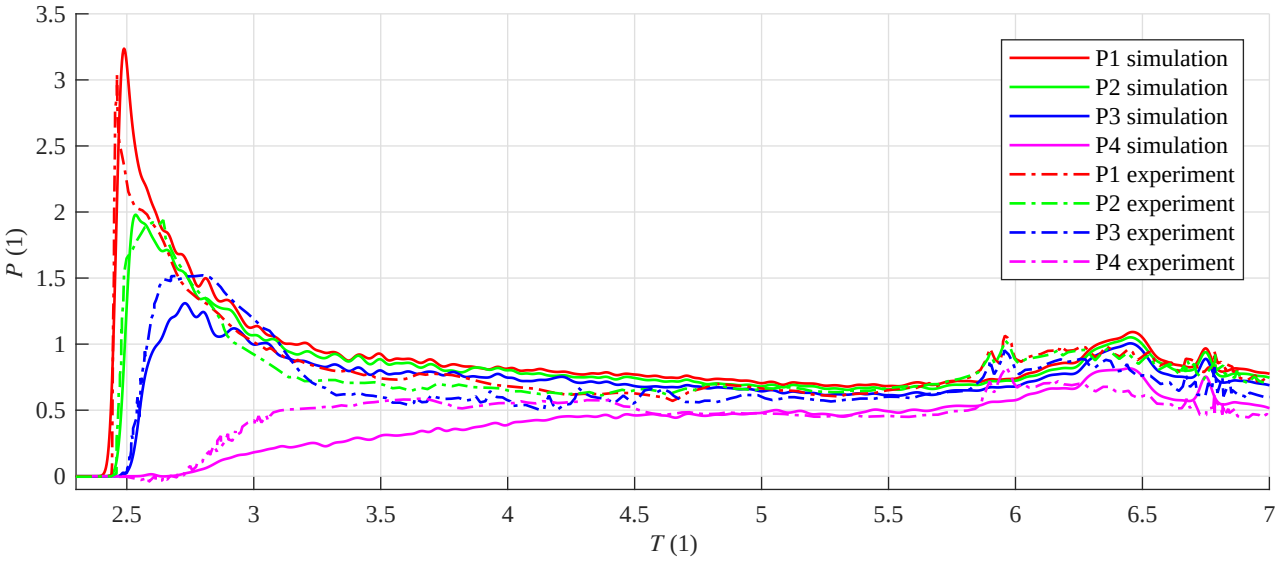

Fig. 2. *Non-dimensional pressure as a function of non-dimensional time at sensors P1 - P4. Comparison of the numerical and the experimental data from [8]*

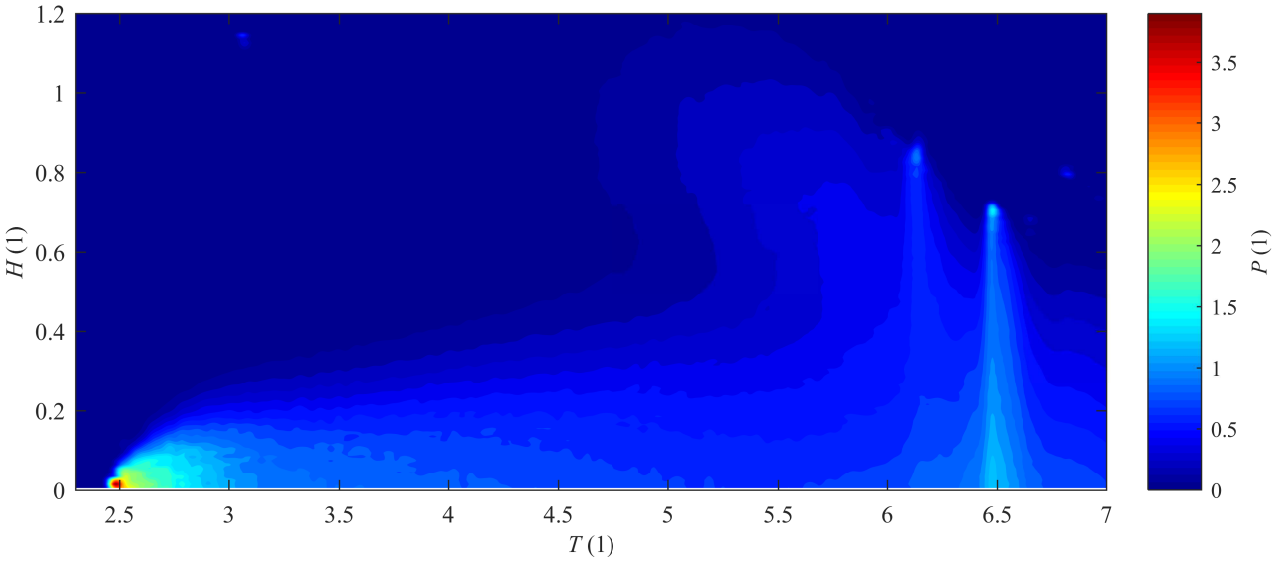

Fig. 4. *Distribution of non-dimensional pressure along the downstream vertical wall as a function of non-dimensional time.*

total force shows when the pressure in the corner is relatively low ($T = 2.80$), but the liquid affected area is already significant (Figure 6). The magnitude of the force peak is less than one half of the hydrostatic force caused by a liquid column of the initial height. A drop in the total force follows as the pressure peak further decreases. However, the pressure affected area of the wall grows fast, and the total force grows together with it. The total force reaches higher a value than the first peak after a while.

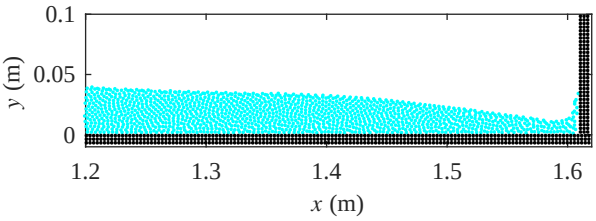

Fig. 5. *Detail of the solution for $T = 2.48$. Pressure reaches its maximal value.*

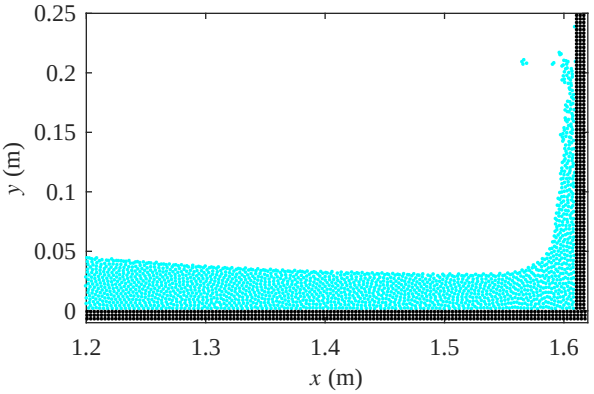

Fig. 6. *Detail of the solution for $T = 2.80$. Total force reaches its first peak.*

The vertical jet gradually loses its momentum, especially its higher parts. However, the liquid from the bottom part of the tank still flows upwards along the vertical wall. Consequently, a bulge of liquid appears on the wall (Figure 7). It leads to a relatively sudden increase in the liquid affected area, and it is well noticeable in the pressure distribution at about $T = 4.6$. On the other hand, this phenomenon does not clearly appear in the evolution of the total force. The total force gradually rises from its local minimum without any noticeable change in its gradient.

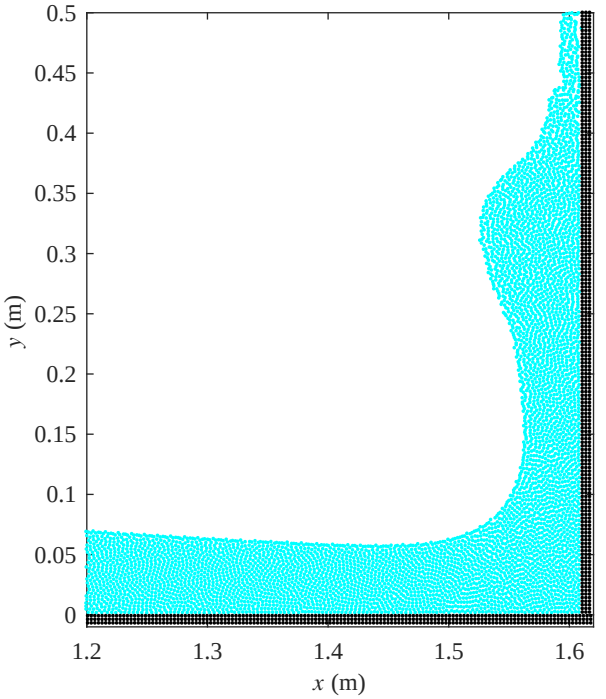

Fig. 7. *Detail of the solution for $T = 4.60$. The bulge on the vertical wall.*

A rolling wave evolves from the bulge as shown if Figure 8. As the tip of the rolling wave approaches the surface, the total force on the wall still gradually increases. Just before the impact, the total force reaches the magnitude about twice as big as the peak

occurring right after the impact. That means that it almost reaches the same magnitude as the hydrostatic force caused by a liquid column of the initial height. The liquid affected area of the wall gradually decreases.

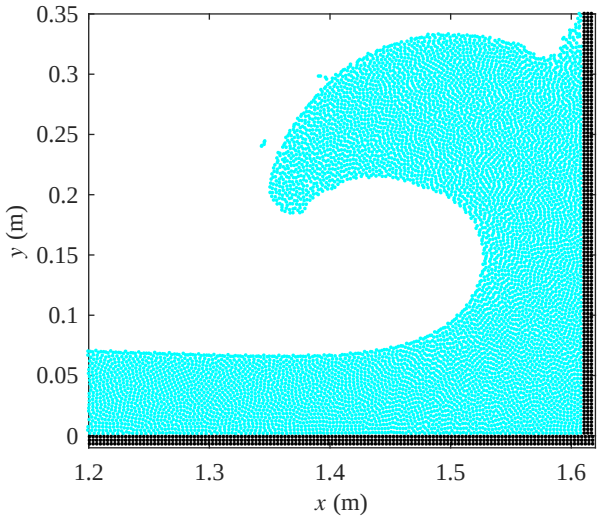

Fig. 8. *Detail of the solution for $T = 5.75$. The rolling wave.*

As the jet further descends, the liquid affected area gradually decreases. There are two significant peaks present at about $T = 6.12$, and $T = 6.50$ in the pressure distribution, and they strongly affect the total force as well. Groups of particles impacting the surface very close to the wall generate these peaks. These particles were ejected from the main fluid body in the initial stage of the surge impact. However, the rise in total force is not caused by these impacts alone. The pressure increases because the flow under the rolling wave accelerates towards the right wall after the rolling wave impacts.

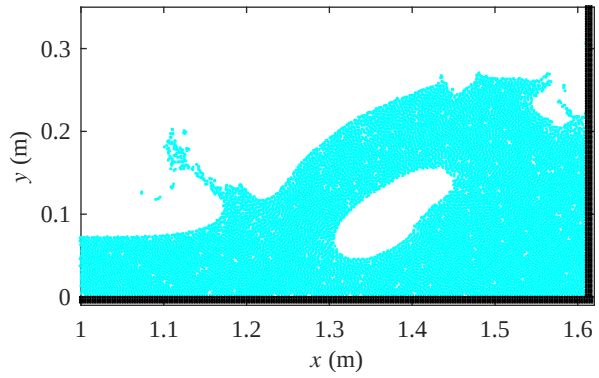

Fig. 9. *Detail of the solution for $T = 6.50$. Increase in total force caused by the accelerated flow under the rolling wave and the impacting particles.*

While the accelerated fluid under the rolling wave is simulated quite well in two dimensions, the impacting groups of particles are questionable. These small groups are likely to shatter into droplets, and their motion is three dimensional. They are also affected by a surrounding gaseous phase and surface tension, which are not modelled in the simulation. However, two-dimensional simplification captures most of the features of the flow well, especially in the early phase of the solution.

4. Conclusion

This paper presents a way of pressure evaluation in the weakly compressible SPH method. It was successfully validated using experimental data from the dam break problem and used to determine the pressure distribution along the downstream vertical wall and the total force acting on this wall during the dam break.

Comparison between experimental and numerical results showed a good agreement, and therefore the proposed model and pressure evaluation technique could be used. The computed pressure distribution and the total force were analysed, and a connection between kinematics and dynamics was investigated. An interesting finding is that there is a peak of total force occurring shortly after the initial impact. However, its magnitude is relatively small compared to the force acting later. Another remarkable discovery is that the pressure peak value appears very shortly after the surge impact, but the maximal total force occurs much later, during the rolling wave impact.

The future work should investigate the influence of the position of the downstream vertical wall on the pressure distribution and the total force. A question is whether these functions change only quantitatively, or if there is a qualitative change at a certain point. Another interesting issue is if there is a distance of the downstream vertical wall at which the total force reaches its extreme value. This information might become useful for designing wave breakers or other structures. Even a relatively simple simulation similar to the one presented here could answer these questions, as illustrates the presented work.

Acknowledgement

This work was supported by the Grant Agency of the Czech Technical University in Prague, grant No. SGS18/124/OHK2/2T/12.

Nomenclature

Subscript indices i and j denote particles, indices m and n denote time steps, index 0 labels reference value, and index S labels sensor.

$\vec{A}$	oriented area vector	(m^2)
c	speed of sound	$(\mathrm{m} \cdot \mathrm{s}^{-1})$
D	artificial diffusion term	$(\mathrm{kg} \cdot \mathrm{m}^{-3} \cdot \mathrm{s}^{-1})$
d	number of spatial dimensions	(1)
$\vec{F}$	force vector	(N)
$\vec{f}$	force per unit mass vector	$(\mathrm{m} \cdot \mathrm{s}^{-2})$
h	smoothing length	(m)
m	mass	(kg)
P	non-dimensional pressure	(1)
p	pressure	(Pa)
R	dimensionless distance	(1)
T	non-dimensional time	(1)
t	time	(s)
$\vec{v}$	velocity vector	$(\mathrm{m} \cdot \mathrm{s}^{-1})$
W	smoothing function	$(\mathrm{m}^{-\mathrm{d}})$
$\vec{x}$	position vector	(m)
Y	non-dimensional horizontal dimension	(1)
y	horizontal dimension	(m)
z	transverse dimension	(m)
γ	equation of state exponent	(1)

δ artificial diffusion coefficient (m^2)
Φ non-dimensional force (1)
Π artificial viscosity term $(\mathrm{kg}^{-1} \cdot \mathrm{m}^5 \cdot \mathrm{s}^{-2})$
ϱ density $(\mathrm{kg} \cdot \mathrm{m}^{-3})$

References

[1] J. C. Martin, W. J. Moyce, W. G. Penney, A. T. Price, and C. K. Thornhill. "Part IV. An experimental study of the collapse of liquid columns on a rigid horizontal plane". In: *Philosophical Transactions of the Royal Society of London A: Mathematical, Physical and Engineering Sciences* 244.882 (1952), pp. 312–324. ISSN: 0080-4614. DOI: 10.1098/rsta.1952.0006.

[2] C. W. Hirt and B. D. Nichols. "Volume of fluid (VOF) method for the dynamics of free boundaries". In: *Journal of Computational Physics* 39.1 (1981), pp. 201–225. ISSN: 0021-9991. DOI: 10.1016/0021-9991(81)90145-5.

[3] J. J. Monaghan. "Simulating free surface flows with SPH". In: *Journal of Computational Physics* 110.2 (1994), pp. 399–406. ISSN: 0021-9991. DOI: https://doi.org/10.1006/jcph.1994.1034.

[4] S. Koshizuka and Y. Oka. "Moving-particle semi-implicit method for fragmentation of incompressible fluid". In: *Nuclear Science and Engineering* 123.3 (1996), pp. 421–434. DOI: 10.13182/NSE96-A24205.

[5] Z. Q. Zhou, J. O. De Kat, and B. Buchner. "A nonlinear 3D approach to simulate green water dynamics on deck". In: *Seventh international conference on numerical ship hydrodynamics*. 1999, pp. 1–4.

[6] K. M. T. Kleefsman, G. Fekken, A. E. P. Veldman, B. Iwanowski, and B. Buchner. "A Volume-of-Fluid based simulation method for wave impact problems". In: *Journal of Computational Physics* 206.1 (2005), pp. 363–393. ISSN: 0021-9991. DOI: 10.1016/j.jcp.2004.12.007.

[7] R. Wemmenhove, R. Gladsø, B. Iwanowski, and M. Lefranc. "Comparison of CFD calculations and experiment for the dambreak experiment with one flexible wall". In: *Proceedings of the International Offshore and Polar Engineering Conference* 3 (2010), pp. 200–205.

[8] L. Lobovský, E. Botia-Vera, F. Castellana, J. Mas-Soler, and A. Souto-Iglesias. "Experimental investigation of dynamic pressure loads during dam break". In: *Journal of Fluids and Structures* 48 (2014), pp. 407–434. ISSN: 0889-9746. DOI: 10.1016/j.jfluidstructs.2014.03.009.

[9] S. Marrone, M. Antuono, A. Colagrossi, G. Colicchio, D. Le Touzé, and G. Graziani. "δ-SPH model for simulating violent impact flows". In: *Computer Methods in Applied Mechanics and Engineering* 200.13 (2011), pp. 1526–1542. ISSN: 0045-7825. DOI: 10.1016/j.cma.2010.12.016.

[10] S. Adami, X. Y. Hu, and N. A. Adams. "A generalized wall boundary condition for smoothed particle hydrodynamics". In: *Journal of Computational Physics* 231.21 (2012), pp. 7057–7075. ISSN: 0021-9991. DOI: 10.1016/j.jcp.2012.05.005.

[11] P. Jančík and T. Hyhlík. "A comparison of two ways of modelling free-slip boundary condition in the SPH method". In: *AIP Conference Proceedings* 2000.1 (2018), p. 20009. ISSN: 0094-243X. DOI: 10.1063/1.5049916.

[12] P. Jančík and T. Hyhlík. "Pressure evaluation during dam break using weakly compressible SPH". In: *Experimental Fluid Mechanics 2018*. Liberec, 2018, pp. 219–224.

[13] G. R. Liu and M. B. Liu. *Smoothed particle hydrodynamics - A meshfree particle method*. World Scientific, 2003. ISBN: 9789812564405.

[14] J. J. Monaghan and R. A. Gingold. "Shock simulation by the particle method SPH". In: *Journal of Computational Physics* 52.2 (1983), pp. 374–389. ISSN: 0021-9991. DOI: 10.1016/0021-9991(83)90036-0.

[15] D. Molteni and A. Colagrossi. "A simple procedure to improve the pressure evaluation in hydrodynamic context using the SPH". In: *Computer Physics Communications* 180.6 (2009), pp. 861–872. ISSN: 0010-4655. DOI: 10.1016/j.cpc.2008.12.004.

[16] A. Colagrossi and M. Landrini. "Numerical simulation of interfacial flows by smoothed particle hydrodynamics". In: *Journal of Computational Physics* 191.2 (2003), pp. 448–475. ISSN: 0021-9991. DOI: 10.1016/S0021-9991(03)00324-3.